Structure and texture of anisotropic nematic gels

P. Gautier,[1,2,]* M. Brunet,[2] J. Grupp,[1] L. Noirez,[3] and E. Anglaret[2]

[1]*Groupe de Dynamique des Phases Condensées, UMR CNRS 5581, Université Montpellier II,
34095 Montpellier Cedex 5, France*
[2]*ASULAB S.A., Rue des Sors, Marin, Switzerland*
[3]*Laboratoire Léon Brillouin, CEA Saclay, UMR CNRS 12, Gif sur Yvette, France*

Anisotropic nematic gels are prepared via *in situ* polymerization of diacrylate monomers in an oriented nematic liquid crystal (LC) matrix. The structure of the gels is studied from micrometer to nanometer scales by optical microscopy, small angle neutron scattering, and $\theta/2\theta$ light scattering. A strong anisotropy is evidenced at all scales without electric field for both mesogenic and nonmesogenic monomers. The gel network can be pictured as an ordered but strongly distorted and polydisperse structure with two characteristic sizes: the mean size of the polymer objects and a correlation length between these objects, corresponding to the mean-size of the LC domains, which are estimated from neutron and light scattering results to be of the order of some tens of nanometers and some micrometers, respectively. Moreover, a sheet-like structure of the polymer network is evidenced. When an electric field is applied, one part of the LC switches while the other part remains anchored to the polymer network. The electric field dependence of the volume fraction of anchored LC is estimated from the analysis of the light scattering data. We emphasize systematic correlations between structure and electro-optical properties of the gels.

PACS number(s): 61.30.Pq

I. INTRODUCTION

The orientation of liquid crystal (LC) molecules at interfaces and in confined geometries is a topic of current interest [1]. Anisotropic nematic gels can be prepared in thin cells via UV photoinduced polymerization of diacrylate monomers (a few mol %) within a nonreactive nematic LC matrix [2]. Aligning layers deposited on the glass windows of the cells leads to a planar and uniform anchoring of the LC on the surfaces and to an overall alignment of the bulk [3]. Polymerization in such an anisotropic matrix leads to an anisotropic polymer network oriented along the LC director. Reciprocally, the LC molecules anchor on the polymer network, which induces drastic changes in the behavior of the LC under electric field. A progressive transition is obtained between the *off* transparent state and the *on* scattering state by applying an ac electric field. The electro-optical properties of such composites were extensively studied [2,4–13]. So far, two possible structures were proposed in the literature [4,7]. They are sketched in Fig. 1. In model 1, the polymer forms thin sheets that interconnect to form cavities oriented along the director axis, in which the LC molecules are confined [Fig. 1(a)] [4,7]. In model 2, the polymer forms oriented cylinderlike fibrils, which assemble into bundles of submicrometer size and are surrounded by interconnected domains of LC [Fig. 1(b)] [2,4]. Hikmet and Boots reported that one can obtain structures corresponding to model 1 or 2 depending on the chemical nature of the monomer and/or their concentration. They studied the switching behavior for both of them and observed two distinct responses [4]. For gels of model 1, each LC domain is separated from the others by polymer sheets and therefore the switching behavior is dominated by the effect of the sheet interfaces. In this case, the

electro-optical characteristic (EOC) is sensitive to the polymer concentration but not to the sample thickness, and no hysteresis is measured in the EOC. By contrast, for gels of model 2, the LC domains are interconnected and therefore switching is dominated by the effect of the cell surfaces. In this case, the EOC does not depend significantly on the polymer concentration but is very sensitive to the cell thickness and a hysteresis is measured in the EOC.

The study of the gel structure is not straightforward in the real space. The anisotropy can be evidenced by optical microscopy between crossed polarizers [4] but the study of the structure at a submicronic scale requires a better resolution. Several groups studied the anisotropy of nematic or cholesteric gels by scanning electron microscopy (SEM) [2,14,15]. The shape and characteristic sizes of the polymer network can be estimated directly from the SEM pictures. Fibril-like or sheetlike structures were observed [14,15]. However, in-
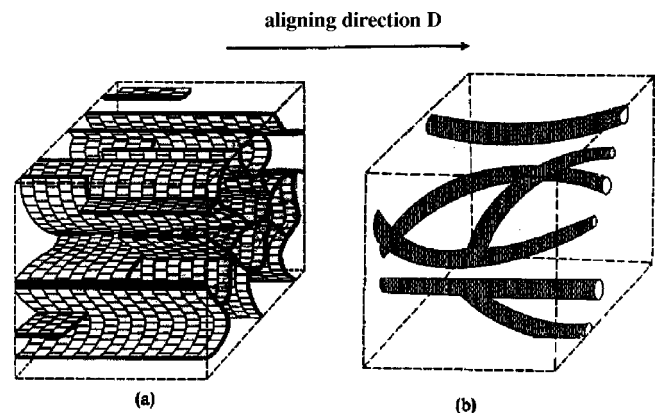

FIG. 1. Sketch of the structure of nematic gels, as proposed by Hikmet and Boots (from Ref. [4]). (a) Interconnected polymer network, hereafter called Hikmet's model 1; (b) independent, cylinder-shaped, polymer objects, hereafter called Hikmet's model 2.

---

*Present address: Optogone S.A., Plouzane, France.

68 011709-1

vestigations by electron microscopy techniques cannot be performed on wet gels. Some studies were performed on dry gels after evacuation of the LC molecules [2]. However, because of possible collapsing by action of capillarity forces, the hypothesis that the polymer network structure is conserved during drying remains questionable.

On the other hand, only a few studies of the structure were performed in the reciprocal space. Braun *et al.* performed small-angle x-ray scattering (SAXS) measurements on wet and dry anisotropic gels [9] and proposed a bicontinuous structure with a characteristic scale of 10 nm to interpret their data. Jàkli *et al.* [11] reported small-angle neutron scattering (SANS) investigations of pastes of polymer LC composites polymerized with the LC in the isotropic or smectic *A* phase. A small anisotropy was evidenced for samples polymerized in the smectic phase under magnetic field. The data were interpreted by assuming a fibrillic structure (Hikmet's model 2), the characteristic mean diameter of the fibrils was estimated to be of the order of some tens of nanometers. To our knowledge, the study of the structure of nematic gels in thin display cells oriented by surface aligning layers was never performed so far by SAXS or SANS. However, the structure of the polymer network at the nanometer scale remains of fundamental importance to improve the electro-optical properties. At the micrometer scale, light scattering was mostly used as a probe of the electro-optical properties [2]. Analytic description of the data is not straightforward because of the polydisperse structure. However, in a recent paper [13], we showed that light scattering experiments can help describing the switching behavior of nematic gels via an estimate of the electric field dependence of the ratio of switched LC. Some questions, however, remained open, for example, the reason why the maximum of scattered intensity shifts to large q when the electric field increases was not well adressed in this former study.

Finally, spectroscopic measurements have provided indirect but relevant informations on the structure of nematic gels. Riede *et al.* performed ^{13}C NMR studies of nematic gels prepared with diacrylate monomers and polymerized under electric field [7]. Their data support the model of nearly cylindrical LC domains surrounded by thin walls of polymer network (Hikmet's model 1). The size of the domains is estimated at about 35 and 100 nm for monomer concentrations of 20 and 8 mol %. On the other hand, Gautier *et al.* showed that one can estimate the ratio of switched molecules from a polarized Raman study, in good agreement with light scattering results [12,13].

In this paper, we study the structure of nematic gels by three different techniques: optical microscopy, SANS, and $\theta/2\theta$ light scattering. We find evidence of strong anisotropy of the polymer network at both nanometer and micrometer scales. We discuss the structural changes under electric field and the different behaviors observed for mesogenic and nonmesogenic monomers. We show that the gels can be characterized by two characteristic scales: the (small) size of the polymer objects and a correlation length between these objects, which also corresponds to the typical transverse size of the LC domains. This allows us to propose a detailed sketch of the structure of the polymeric network in nematic gels and
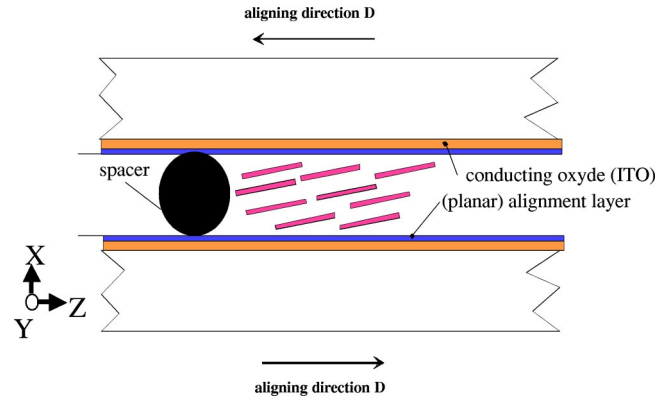

FIG. 2. Sketch of a cell and definition of the reference frame. Z corresponds to the aligning direction, X to the cell thickness.

of the switching of the LC under electric field. Finally, we discuss the correlations between the structure and the electro-optical properties of nematic gels.

II. EXPERIMENT

A. Preparation of the samples

The preparation of the gels was described in detail elsewhere [12,13]. Briefly, the gels were prepared using the liquid crystal E7 (essentially a mixture of cyanobiphenyls and cyanoterphenyl, nematic between $-10\,°C$ and $60.5\,°C$) from Merck and 0.5–3 mol % of a fluorinated dimethacrylate mesogen monomer, hereafter called 4d, or of a nonfluorinated diacrylate nonmesogenic monomer, hereafter called 6bab, both synthesized by T. Chuard and R. Deschenaux at Institut de Chimie, Université de Neuchâtel. Common LC thin display cells were prepared with two parallel glass plates recovered by transparent ITO electrodes and coated with a thin film of polyimide (see sketch in Fig. 2). The film was rubbed with velvet in order to induce planar alignment of the LC molecules [3]. For some cells, homeotropic alignment was achieved from a special polyimide coating without rubbing. Spacers were used to obtain well-controled and uniform thickness. The thickness was fixed to about 9 μm for light experiments and electro-optical studies. The cells were filled at room temperature by capillarity and then exposed to UV light for several hours. The conversion rate of monomers was determined from Fourier transform infrared (FTIR) measurements and found to range between 50% and 80% [16]. The light transmission for as-prepared gels was between 80% and 90%. In the following, we will associate the following reference frame to the cells prepared with planar alignment: Z corresponds to the aligning direction, X corresponds to the thickness, and Y corresponds to the third dimension (Fig. 2).

B. Optical microscopy measurements

The samples have been studied by optical microscopy between crossed polarizers at various temperatures. The results for a gel prepared with 1.1 mol % of 4d are displayed in Fig. 3. Picture 3(a) shows the picture of the gel at room temperature, with the aligning direction $\vec{D}$ parallel to the polarizer.
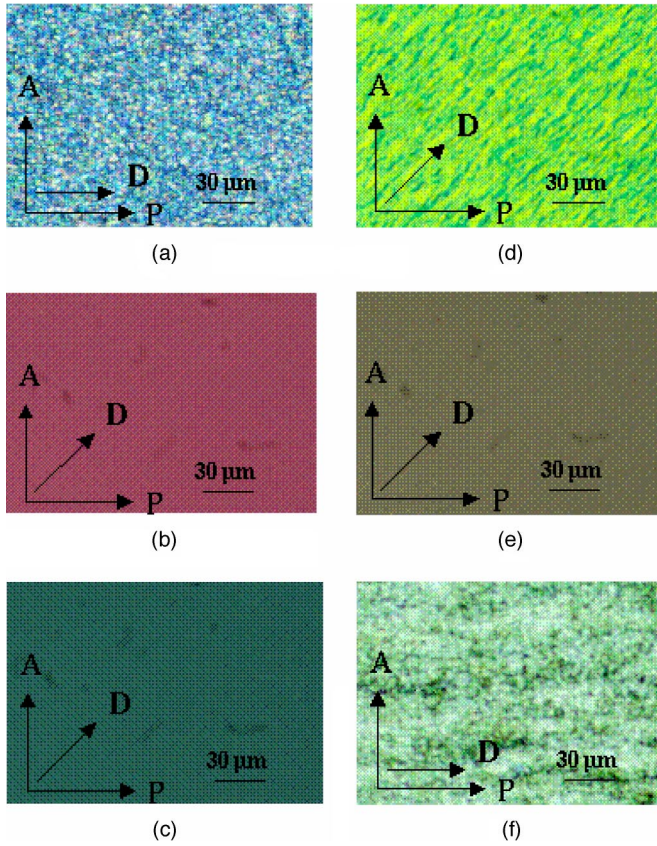
FIG. 3. (Color online) Optical microscopy pictures between crossed polarizers (in the ZY plane) of a gel prepared with 1.1% mol of monomer 4d. (a) Aligning direction parallel to the polarizer, room temperature, (b)–(e) aligning direction at 45° from the polarizer, $T = T_{NI} - 45\,°C$, $T = T_{NI} - 8\,°C$, $T = T_{NI} - 5\,°C$, $T = T_{NI} + 5\,°C$, respectively, (f) aligning direction parallel to the polarizer, $T = T_{NI} + 5\,°C$.

The texture is non uniform, it presents both colored and dark domains, with typical sizes of about $1-1.5$ μm. Note that in the same configuration, an uniform cell of nematic LC would be completely black. Pictures 3(b)–3(e) were observed as a function of temperature, after rotation of the cell of 45°. At room temperature [Fig. 3(b)] no texture can be observed. It proves that in the domains of picture 3(a), the director deviates only a little from $\vec{D}$. Otherwise, some of the domains would be extinguished at 45° and the texture would still be visible. The observed color is related to the optical retardation, $\delta = \Delta n e$, where Δn is the birefringence and e the cell thickness (here, $e \simeq 10$ μm). The birefringence of a LC decreases as the temperature increases, and reaches 0 at T_{NI}. The observed change of colors is due to the variation of δ, connected to the variation of Δn, and can be controlled on the Newton scale. The color we observed for this gel at room temperature ($T = T_{NI} - 45\,°C$) was a pale pink of the fifth order [Fig. 3(b)], which corresponds to a retardation of about 2000 nm and therefore a birefringence of about 0.2. At $T = T_{NI} - 8\,°C$ [picture 3(c)], the color is green of the second order ($\delta \simeq 700$ nm and $\Delta n \simeq 0.07$). At $T = T_{NI} - 5\,°C$ [picture 3(d)], an anisotropic texture is observable, with the anisotropic axis oriented parallel to the aligning direction.

Here, the contrast is due to a different evolution of the birefringence, probably weak for the polymer but steep for the LC near the transition. The typical distance between domains is of the same order as the domain size evaluated from picture 3(a). We will see below that this typical distance is also of the same order than that measured by light scattering. Finally, at $T = T_{NI}$ and above, the anisotropic texture disappears and a small retardation is observable [picture 1(e)], corresponding to a gray of the first order ($\delta \simeq 200$ nm and $\Delta n \simeq 0.02$). This residual retardation when the nematic matrix is isotropic is certainly due to the residual birefringence of the oriented polymer network, and possibly also to the birefringence of oriented LC domains anchored on the network. Note that for a LC above T_{NI}, $\delta = 0$ and the field would be black. Finally, when the cell is observed with $\vec{D}$ parallel to the polarizer above T_{NI} [picture 3(f)], there is no extinction as it would be for the bulk but again a texture, slightly anisotropic and different than that observed at room temperature on picture 3(a). This texture and the residual birefringence indicate an alignment of the polymer network along $\vec{D}$. Note that the texture is very different than that observed by Hikmet and Boots on gels with fibrillic structure (Hikmet's model 2). By contrast, it seems rather close to what was observed for gels of model 1 [4].

In summary, these optical microscopy measurements allow us to evidence the anisotropic texture of the gels at the micrometer scale. Note that the anisotropy is more easily observable for smaller concentrations and/or nonmesogenic monomer (not shown) because the typical size between oriented domains increases. We show below that the typical sizes measured in microscopy are in good agreement with light scattering results.

C. Small-angle neutron scattering experiments

Specific cells were prepared for neutron studies in order to optimize the scattered signal. High-purity quartz windows were used to avoid neutron absorption by bore impurities. The conducting ITO layer was replaced by a thin layer (10 nm) of nickel to avoid absorption by indium. The thickness of the cells was fixed to 175 μm and each experiment was achieved on a set of two superimposed cells. This procedure allows us to improve the scattered signal and to preserve a good (layer-induced) alignment of the LC. In order to increase the scattering contrast, the main component of the E7, 5CB, was deuterated (by courtesy of P. Keller, Institut Curie, Paris). We checked that the scattering from empty cells and from bulk deuterated LC was negligible with respect to scattering from gels. Therefore, the scattering contrast is produced by the difference of scattering density between the polymer phase and the LC phase. Four samples were studied: two with the monomer 4d and two with the monomer 6bab. The monomer concentrations were 0.7 and 1.5 mol %.

SANS experiments were performed at Laboratoire Léon Brillouin on the spectrometer PAXY. Different wavelengths and sample-to-detector distances were used to cover the scattering range $5 \times 10^{-3} - 4 \times 10^{-2}$ Å^{-1}.

D. $\theta/2\theta$ elastic light scattering experiments

The structure of the gels was also investigated in elastic light scattering experiments, using a monochromatic incident radiation of wavelength 1 μm. The scattering intensities were corrected from Fresnel reflections and angular dependent beam path. We used a $\theta/2\theta$ setup in order to keep the scattering vector $\vec{q}$ in the plane of the substrates.

III. RESULTS AND INTERPRETATION

A. Anisotropy of the polymer network

Neutron scattering patterns display strongly anisotropic shapes for all samples studied. Typical patterns without electric field are displayed in Fig. 4(a) and in the left part of Fig. 5. The scattering signal is very anisotropic being much more extended along the direction (Y) perpendicular to the aligning direction. This indicates that fluctuations of the scattering length are preferentially in this direction and therefore that the polymer network orients preferentially parallel to the aligning direction. For both mesogenic and nonmesogenic monomers, this anisotropy is a direct evidence that polymerization in an oriented nematic solvent induces an orientation of the polymer network parallel to the nematic director. Note that for the same molecular fraction of monomer (0.7%), the SANS anisotropy is smaller for the gel prepared with nonmesogenic monomers (Fig. 5, bottom left). In addition, the very weak signal measured in the direction parallel to the aligning direction (Z) indicates that there are essentially no length scattering density fluctuations in this direction. By contrast, an isotropic pattern is observed in the plane perpendicular to the aligning direction for gels prepared with homeotropic alignment [Fig. 4(b)]. Assuming that the growth of the polymer network is comparable for cells prepared with planar and homeotropic anchoring, this indicates that the polymer network displays an anisotropic structure oriented along the aligning direction and presents a cylindrical symmetry with respect to this direction.

The anisotropy of the polymer network was also probed under application of an ac electric field. The changes in the scattering pattern are displayed in Fig. 5 for an electric field of 2.3 V μm^{-1}. Essentially no change is observed for gels prepared with the mesogenic monomer 4d. By contrast, applying an electric field leads to a significant loss of the SANS anisotropy for gels prepared with the nonmesogenic monomer 6bab (Fig. 4 bottom). This change is irreversible and the original pattern is not recovered once the electric field is released. This indicates an irreversible deformation of the polymer network in 6bab gels induced by the electric field. This deformation cannot be assigned to a direct electro-optical effect, since the monomer has no mesomorphic properties but rather to an hydrodynamic effect. Moreover, since no deformation is observed for the 4d gels, we conclude that 6bab polymer networks present much weaker mechanical properties due to a smaller polymerization rate, and a concomitant smaller reticulation rate. As estimated from infrared studies [16], the conversion rate during polymerization is about 75% and 50% for gels prepared with 0.7 mol% mono-
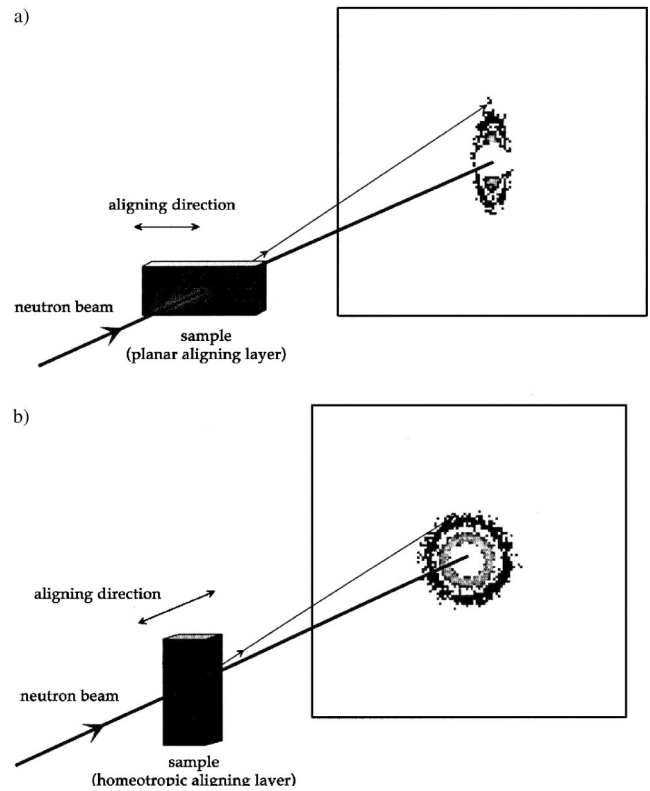
a)

b)

FIG. 4. SANS patterns for a gel prepared with 0.7 mol% of monomer 4d: (a) planar anchoring, scattering in the plane (YZ), (b) homeotropic anchoring, scattering in the plane perpendicular to the aligning direction.

mer of 4d and 6bab, respectively [Figs. 5(a) and 5(b), respectively].

B. Microscopic structure of the polymer network

The quantitative analysis of scattering patterns can provide structural information on the shape, size, and surface roughness of the scattering objects at a scale q^{-1}. SANS experiments give typically access to sizes from the nanometer scale to a few hundreds of nanometers. Let us call a the typical size of the scattering object (the thickness of the sheets in Hikmet's model 1 or the radius of the fibers in Hikmet's model 2) and ξ the typical distance between the scattering objects. If $qa \gg 1$, the SANS pattern will essentially correspond to scattering from the surface of the polymer objects (form factor) and will follow a typical power law, the so-called Porod law $I \simeq q^{-4}$ for smooth interfaces, or $I \simeq q^{-s}$ with $3 \leq s < 4$ for rough or fractal interfaces [18]. If $qa \ll 1$, the SANS signal will be sensitive to the position correlations of the objects. For uncorrelated diluted systems, the signal is expected to be constant (independent of q). For correlated systems, one measures the structure factor of the system (note that for nematic gels, relevant information on the structure factor has also been measured by light scattering and will be presented elsewhere). If now $qa \simeq 1$, a can be estimated within the SANS range. For diluted sytems, the scattering signal corresponds to the form factor of a single object, which is well described by the so-called Guinier ap-
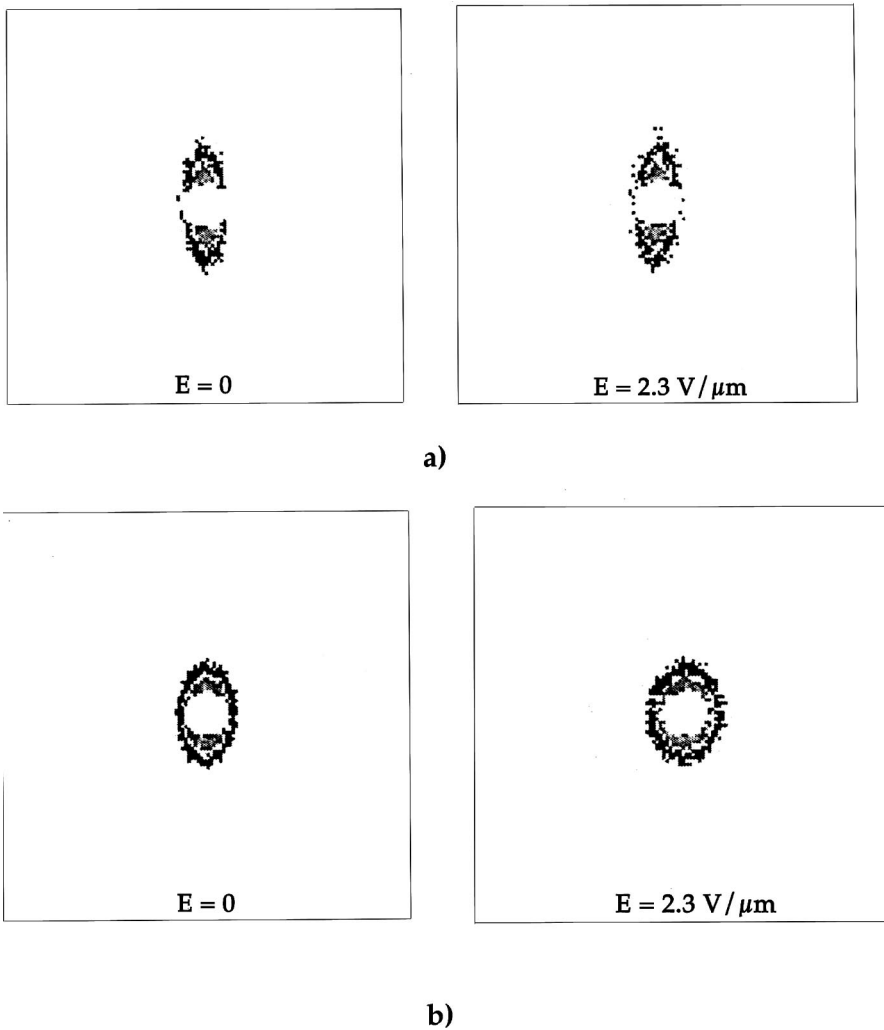
a)

b)

FIG. 5. SANS patterns in the YZ plane (Z is horizontal) for (a) a gel prepared with 0.7 mol % of 4d and (b) a gel prepared with 0.7 mol % of 6bab, without electric field (left) and with an electric field of 2.3 V μm^{-1} (right).

proximation $I(q) \propto \exp(-q^2 R_g^2/3)$, where R_g is the gyration radius, independent of the shape of the scattering objects. For correlated-concentrated systems, the typical size can be estimated from the crossover between two scattering ranges: the form factor at large q and the structure factor at small q.

The scattering signal measured for q parallel to the aligning direction (Z) is restricted to very small q values. No typical size can be determined in this direction in agreement with the picture of long anisotropic LC and polymer objects aligned along the aligning direction. By contrast, an intense and strongly q-dependent scattering signal is measured in the Y direction. The q_Y-dependence of the signal (see an example in Fig. 6) is well fitted by a power law for all samples with a power exponent between 2.3 and 2.7, somewhat intermediate between the two expected limits (Guinier and Porod behaviors). Two interpretations can be proposed: (1) The size of the polymer objects is small and does not contribute to the available SANS q range ($qa \ll 1$) and, therefore, one measures mainly the contribution of the polymer network at scales between $1/a$ and $1/\xi$. Several models of connected networks could explain this power law [17], but it is speculative to go further in the interpretation of the power law given the likely strong polydispersity of the samples. (2) The size of the polymer objects give rise to a scattering in the available SANS q range ($qa \simeq 1$) and, therefore, the data must be considered as a mixed response. Therefore, we propose to decompose the signal into two components corresponding to large and small q behaviors, using for this assumption a two dimensional fit of the SANS figures. Good fits of all sets of data were achieved, using the sum of a power law and a Guinier function. A typical fit of the data for q parallel to Y is presented in Fig. 6. The power law (exponent around 3) dominates the signal at small q and corresponds, therefore, to the high-q part of the structure factor of a correlated system. The Guinier function corresponds to the low-q part of the form factor of the polymer objects. One can estimate the typical size of the objects from the Guinier law. One finds $a \simeq 600$ Å for gels prepared with 1.5 mol % and $a \simeq 900$ Å for 0.7 mol % monomer. Since the size increases when the monomer concentration decreases, it is very likely that the polymer objects are swelled by LC molecules. No significant difference is found between gels prepared with 4d and 6bab monomers for a same monomer concentration. By contrast, significant changes are found for 6bab gels when an electric field is applied and once the electric field is released. This is concomitant with the decrease of anisotropy of the scattering pattern discussed above, and this confirms that the polymer network is partially deformed under electric field
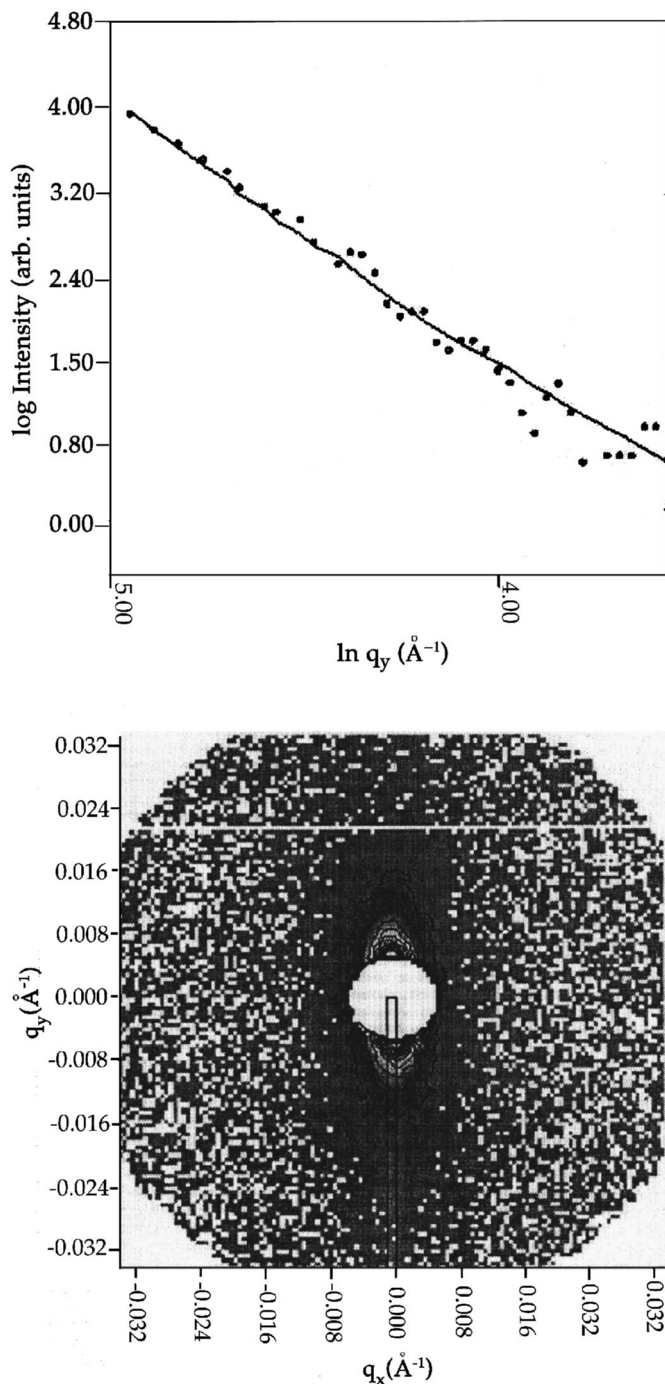
FIG. 6. Typical fit of the SANS data in the Y direction (area framed on the bottom part of the figure) with the sum of a power law and a Guinier function. Here, the data correspond to a gel prepared with 1.5 wt % of monomer 4d.

for 6bab gels. Much weaker changes are observed under electric field for 4d gels and the typical size measured after the field is released is the same as that measured for as-prepared gels.

Complementary measurements would be useful at larger q to confirm the superposition of two contributions. Unfortunately, this is prevented here by the rather strong incoherent scattering signal from the gels, mainly due to the hydrogen

atoms, and they could be performed only with a completely deuterated LC. On the basis of the present experiments, one can, however, state that anisotropic polymer objects are oriented parallel to the aligning direction and that these polymer objects form a network. This rules out the picture of polymer fibers independent from each other. This is rather in agreement with a polymer network made of entangled sheets, close to Hikmet's model 1. The polymer sheets are likely swelled of LC molecules and their typical thickness is at most of the order of some tens of nm. The correlations between sheets extend above the larger scale (some tens of nm) studied in our SANS experiments. We will show in the next part that a correlation length ξ can be measured by light scattering and associated to the typical distance between polymer sheets or, equivalently, to the typical transverse size of the LC domains. A sketch of the proposed structure is presented in Fig. 7.

C. Mesoscopic structure of the polymer network

The SANS studies were completed at smaller q by elastic light scattering experiments. The $\theta/2\theta$ setup allows us to study the polarizability fluctuations in a given direction of the reciprocal space $\vec{q}$ as a function of scattering angle, i.e., as a function of $\|\vec{q}\|$. For near infrared light, one investigates the structures at the micrometer length scale. Contrary to the SANS experiments, the scattering contrast is not provided by the difference of coherent scattering lengths of the LC and the polymer. Here, the contrast is produced by polarizability fluctuations in the gel, which are negligible without electric field (transparent *off* state) and which become important under electric field (scattering *on* state). This electric field-induced contrast occurs between switched LC domains and LC domains anchored to the polymer network [13], as sketched in Fig. 8. For $\vec{q}$ parallel to the aligning direction, scattering remains very weak under electric field [12,13]. This indicates that there is no polarizability fluctuation, i.e., no refractive index fluctuation, in this direction. This is an additional evidence that the polymer objects, and therefore the LC domains (both switched and anchored), are well oriented along the aligning direction. For $\vec{q}$ perpendicular to the aligning direction (parallel to Y), the scattering intensity depends strongly on light polarization [12,13]. For light polarization perpendicular to the aligning direction, scattering remains very weak under electric field. This indicates that there is no refractive index fluctuations along Y and therefore that LC molecules switch in the plane (ZX). In contrast, for light polarized parallel to the aligning direction (or similarly for unpolarized light), an intense and broad scattering peak is measured above a concentration-dependent voltage threshold. Typical scattering patterns for various voltages are presented in Fig. 9, for gels prepared with monomer 4d [Fig. 9(a)] or 6bab [Fig. 9(b)]. The maximum of the peak shifts to high q when the voltage increases while its intensity increases. For some gels, the intensity goes through a maximum at a concentration-dependent voltage and then decreases [Fig. 9(b)]. The position q_0 of the maximum and the full width at half maximum (FWHM) Δq of the peak are
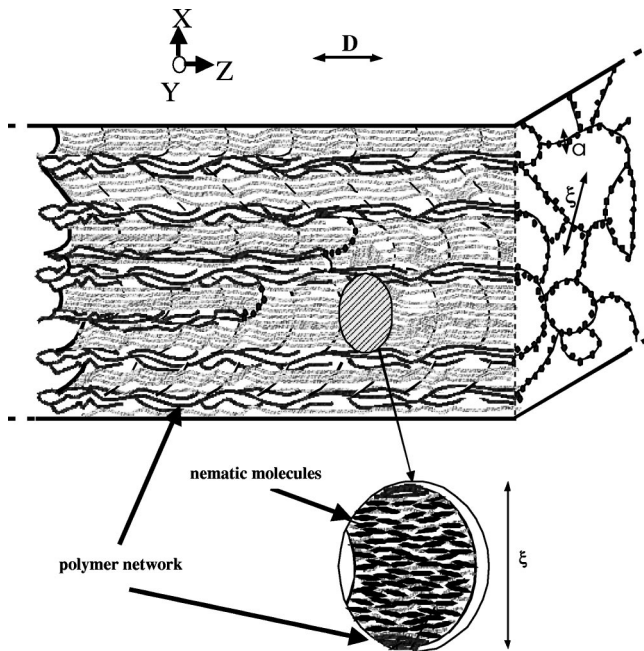
FIG. 7. Sketch of the structure of nematic gels. a is the typical thickness of the polymer sheets, ξ is the correlation length between polymer sheets, or, equivalently, the mean-size of the LC domains.

reported in Fig. 10 for various concentrations of monomers 4d or 6bab. When the concentration of monomers increases, the peak is systematically shifted to large q and broadens slightly. For a same monomer concentration, the peak is downshifted for gels prepared with monomer 6bab with respect to gels prepared with monomer 4d. For the gels prepared with the smallest concentration of 6bab (1 mol %), the position and the width do not follow a monotonous field dependence. This is another signature of the deformation of the polymer network for these gels, and of their concomitant irreversible electro-optical behaviors. Note finally that the
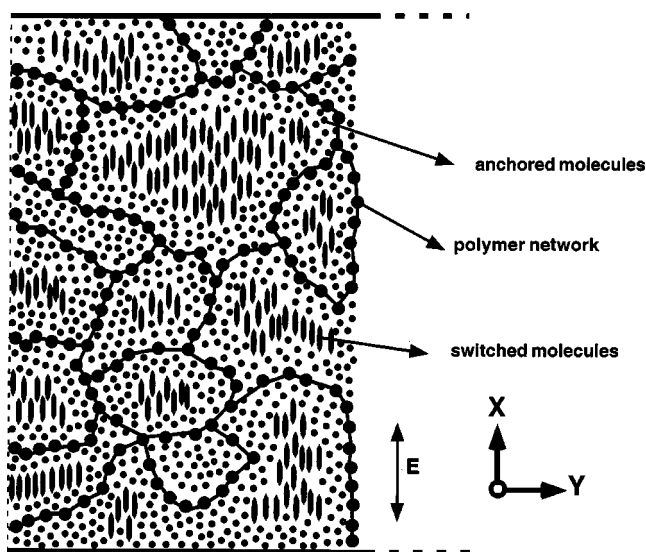

FIG. 8. Sketch of the switching of LC under voltage. The molecules that are close to the cell surfaces and to the polymer interfaces do not switch.
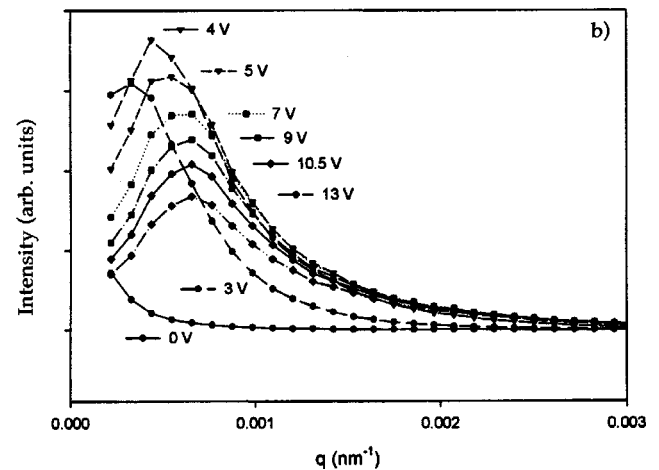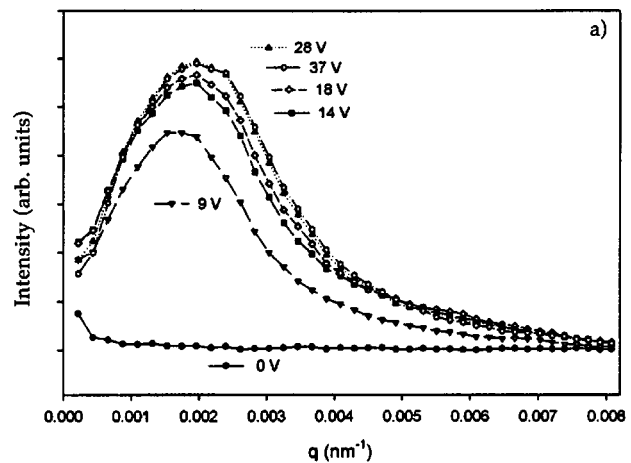

FIG. 9. $\theta/2\theta$ light scattering data for different voltages for a gel prepared with (a) 1 mol % of monomer 4d and (b) 1 mol % of monomer 6bab. The scattering vector is parallel to Y and the light polarization is parallel to the aligning direction Z.

light scattering signal is strongly dependent on the sample thickness (not shown): for thick samples (100 μm or more), the scattering peak is much broader and the maximum is ill defined.

This scattering peak must be associated to a correlation length, which we call ξ and we assign to a typical distance between polymer objects or, equivalently, a typical size of the LC domains. First let us try to interpret the shift of the peak maximum to large scattering vectors with increasing voltage. This may be assigned in part to multiple scattering, which may also explain in part the slight broadening of the peak at large voltages. However, multiple scattering can be neglected at low voltages (large transmissions) while the most important part of the shift occurs in this range (Figs. 9 and 10). Therefore, we rather believe that the shift of the peak reflects the variation of the correlation length as a function of voltage. SANS experiments showed that the structure and anisotropy of the polymer network are not modified under electric field for gels prepared with monomer 4d, and only modified at large voltages for gels prepared with monomer 6bab. Consequently, we rule out the hypothesis of deformation of the polymer network to explain the changes of
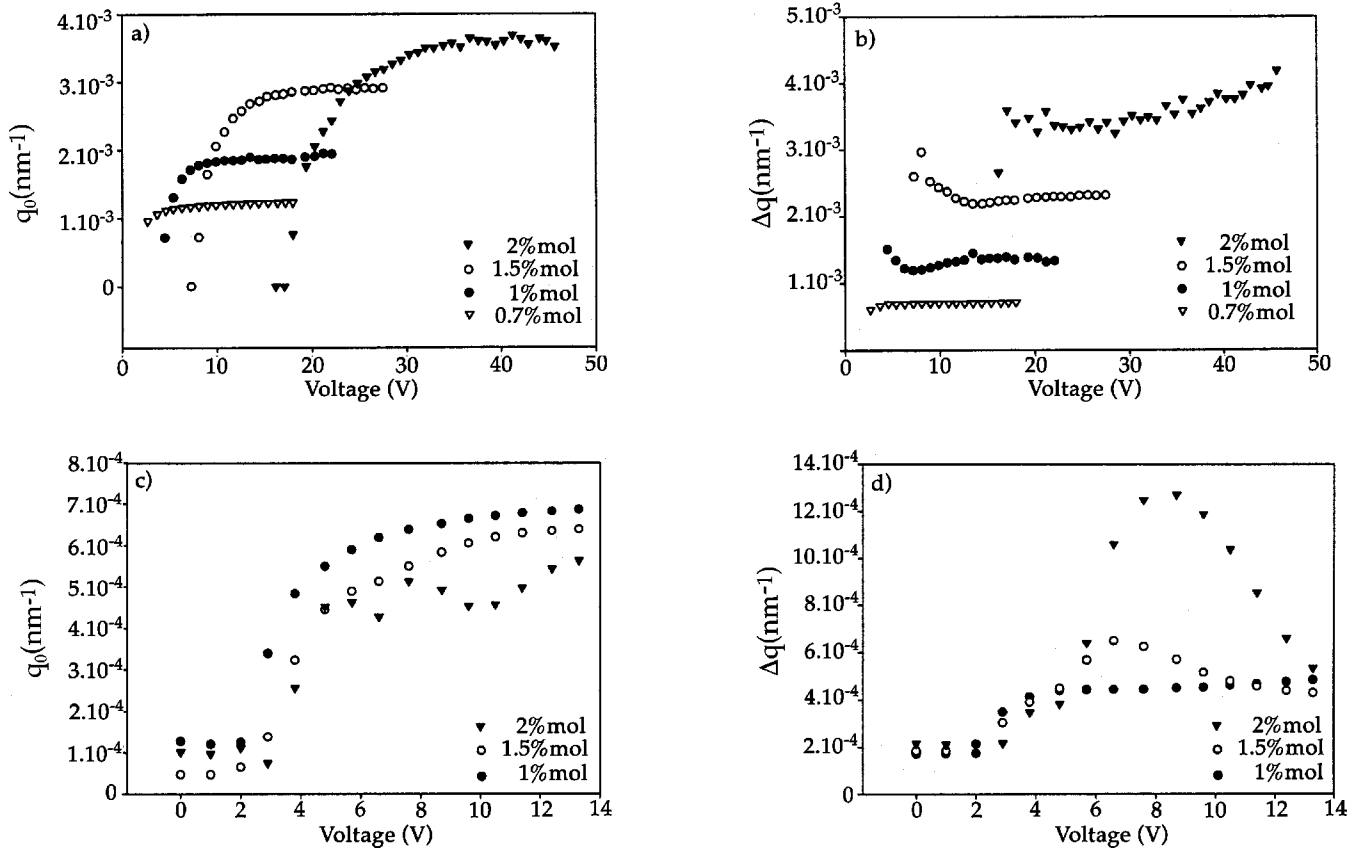
FIG. 10. Voltage dependence of the position q_0 (left) and the width Δq (right) of the scattering peak, as determined from a Lorentzian fit of the data, for (a) gels prepared with monomer 4d, and (b) gels prepared with monomer 6bab.

the peak profile. We rather believe that the upshift of the scattering peak for increasing fields can be explained by a progressive *revealing* of the network structure. We remind here that the scattering contrast is between the switched LC domains and the LC domains anchored to the polymer network. At the switching threshold, only the molecules, which are weakly anchored to the polymer network, i.e., which are most distant from the polymer interfaces, are allowed to switch. The transmission begins to decrease at low voltages, when sufficiently large LC domains are switched. Therefore, the scattering peak at low voltages corresponds to the correlation length between LC domains sufficiently distant from the interfaces. When the voltage increases, other LC domains, closer to the interfaces, are allowed to switch. This voltage dependence of the structure *revealing* is sketched in Fig. 11(a). Therefore, the correlation length between the switched domains decreases when the voltage increases, which induces a shift to large angles of the scattering peak. This voltage dependence of the shift is the signature of a polydisperse structure with a distribution of sizes of the LC domains, and the larger the range of voltages over which the peak shift is observed, the larger the polydispersity. Above a given voltage, the peak position becomes independent of voltage (Fig. 10). Only the intensity of the peak continues to change, indicating an increase of the volume fraction of switched LC *without* changes in the correlation length. Therefore, ξ must be estimated at large voltages, and is of

the order of $2\pi/q_{0_{max}}$, i.e., about 6 μm and 2 μm for 4d gels of concentration 0.7 mol % and 1.5 mol %, respectively, and about 9 μm for 6bab gels of concentration 1.5 mol %. The scattering peak is shifted below the experimental resolution for 6bab gels of concentration 0.7 mol %. A decrease of the correlation length for increasing monomer concentrations was expected, this is the signature of a denser packing of polymer objects. The difference between monomers 4d and 6bab can also be explained in part by a difference of packing density: 6bab gels present smaller polymerization rates and therefore the polymer concentration is smaller for the same monomer concentration.

Even though the analytic description of the angular dependence is not straightforward, one can get a general picture of the structural changes under electric field through the measurement of the total energy scattered by the system, the so-called Porod invariant. Such an analysis was proposed in a previous study [13] and allowed us to estimate the electric field dependence of the volume fractions of switched and anchored LC. The results were shown to be in good agreement with Raman scattering results on the same samples. Figure 12 displays the voltage dependence of the volume fraction of anchored LC ϕ_a for different samples. For each sample, ϕ_a begins to decrease above a first threshold voltage and reaches a plateau above a second threshold voltage. The threshold voltages and the anchored volume fraction at the
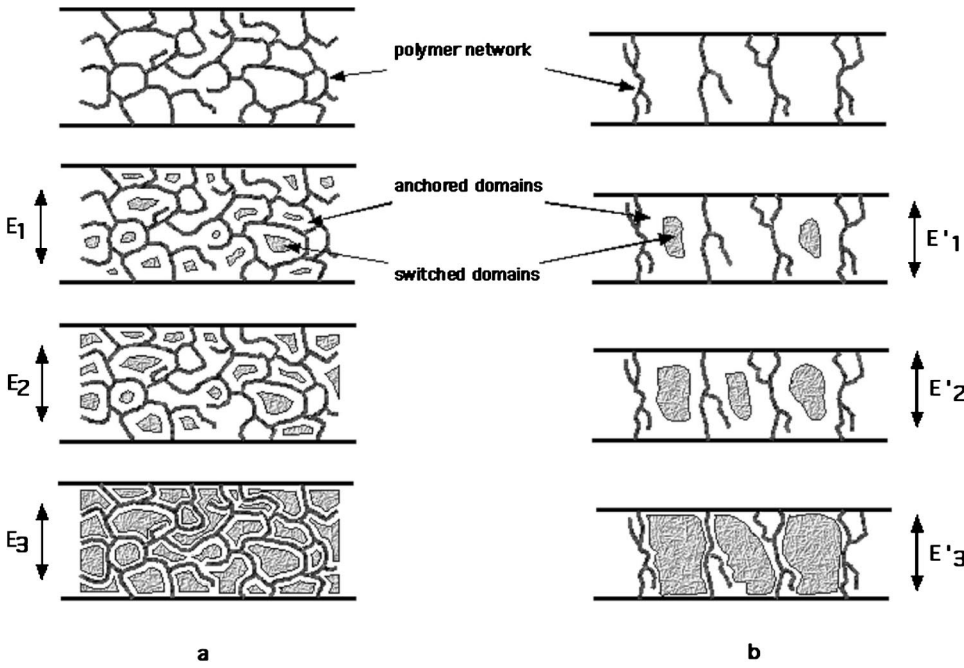
FIG. 11. Sketches of the switching of LC in the XY plane (X is vertical) under increasing voltages. (a) Large monomer concentrations and/or thick cells, (b) small monomer concentrations in thin cells. Top pictures are without electric field. From top to bottom, the electric field is increasing.

plateau $\phi_{a_{min}}$ depend on both the monomer and its concentration : the larger the concentration, the larger the threshold voltages and $\phi_{a_{min}}$. The voltage dependence of ϕ_a is strongly correlated to the electro-optical characteristics of the gels [13].

The alignment of the polymer network parallel to the aligning direction is now well established. For small monomer concentrations, we also observed an anisotropy in the plane (XY), i.e., an alignment of the network perpendicular to the cell surfaces (perpendicular to Y). This can be studied by performing so-called θ measurements, i.e., measurements as a function of the angle θ between the incident beam and the normal to the cell, for a fixed value of the detector position 2θ (corresponding to the maximum of the scattering peak). The stronger the θ dependence of the signal, the stronger the anisotropy: a monocristal would be characterized by a narrow peak in a θ experiment, while the signal would be independent of θ for a powder. The results for the series of gels prepared with monomer 4d are presented in Fig. 13. They are very dependent on the monomer concentration: the smaller the concentration, the larger the anisotropy. For the less concentrated gel (0.7 mol %), the maximum of intensity is well marked at $\theta = 0$. This indicates that the polymer objects are very anisotropic in the plane (XY) and that the correlation length can be defined only along the Y direction. The cristallographic analogy would be a 1D crystal with a cell parameter ξ. By contrast, for the most concentrated gel, the scattering intensity is almost independent of θ and the cristallographic analogy would be a crystalline powder with a cell parameter ξ. Textural differences between gels prepared with large and small monomer concentrations are schematized in Figs. 11(a) and 11(b), respectively. This change of anisotropy with monomer concentration is a striking result. It is obviously related to finite-size effects for small monomer concentrations. Indeed, the correlation length is of the same order of magnitude as the cell thickness for these samples.
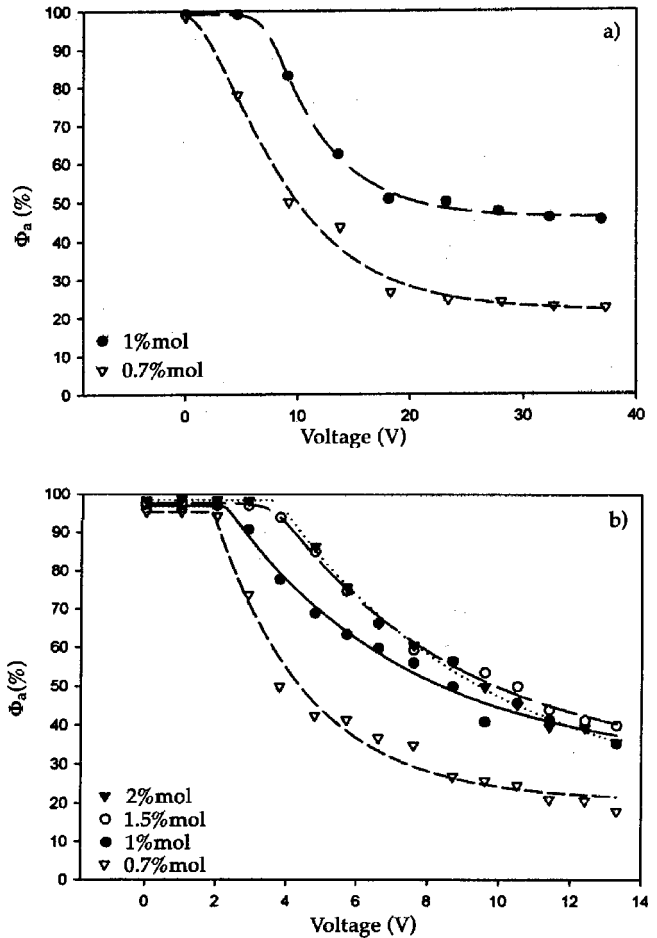

FIG. 12. Voltage dependence of the volume fraction of anchored LC, as determined from the measurement of the Porod invariant on the light scattering data. (a) Gels prepared with monomer 4d, (b) gels prepared with monomer 6bab. The lines are guides for the eyes.
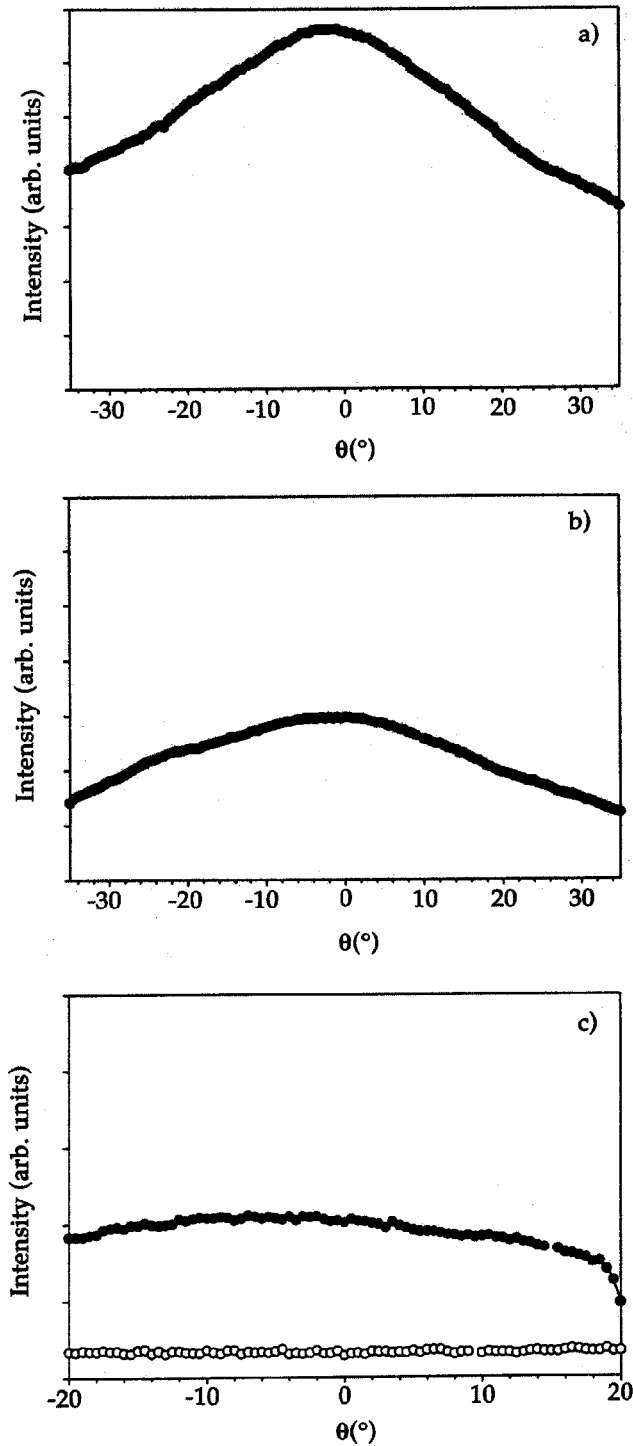
FIG. 13. θ measurements for gels prepared with monomer 4d and different concentrations: (a) 0.7 mol %, (b) 1 mol %, (c) 1.5 mol % (top) and 2 mol % (bottom). The detector is fixed at the angle 2θ corresponding to the maximum of intensity on $\theta/2\theta$ scans. $\theta=0$ corresponds to the maximum of intensity on $\theta/2\theta$ scans.

This suggests that the growth of the polymer network is intrinsically isotropic in the plane perpendicular to the aligning direction, i.e., with a cylindrical symmetry with respect to Z, and is only hindered by the cell windows. This is confirmed by the SANS results performed on relatively thick

cells and/or on cells with an homeotropic anchoring. Note also that the strong broadening of the light scattering peak for thick cells indicates a much less ordered structure at the mesoscopic scale, i.e., a much ill-defined correlation length.

IV. DISCUSSION

Let us first summarize the structural results obtained and propose a schematic description of the nematic gel structure (without electric field). SANS measurements allowed us to evidence the anisotropy of the polymer network at a microscopic (nanometric) scale. The transverse characteristic length of the polymer objects that form the network was estimated to a few tens of nanometers at most. The anisotropy was also observed at a mesoscopic (micrometric) scale by optical microscopy and light scattering: the absence of light scattering when no electric field is applied indicates that there is essentially no polarizability fluctuation, i.e., no refractive index fluctuation at the micrometer scale, which supports the picture of a uniformly oriented network. Consequently, the mesoscopic structure is only revealed when switched LC domains induce a scattering contrast under electric field. This structure is relatively well ordered, especially for low monomer concentrations and thin samples. The correlation length between the polymer objects if of the order of a few micrometers and it decreases when the monomer concentration increases. The polydispersity, i.e., the distribution of sizes of the LC domains is expressed through the width of the light scattering peak and also through the shift of the peak maximum as a function of voltage. The larger the monomer concentration and the sample thickness, the larger the polydispersity. What about the shape of the polymer objects?

(1) The EOC depends strongly on the monomer concentration, which indicates an interconnected polymer network.

(2) The polymer network aligns perpendicular to cell surfaces for low monomer concentrations and thin samples: such an anisotropy is not compatible with a cylindrical symmetry. This rules out the model of independent, cylinder-shaped, polymer objects [Hikmet's model 2, Fig. 1(b)]. By contrast, our results support well the model of entangled polymer sheets, close to Hikmet's model 1 [Fig. 1(a)]. In this model, the polymer network forms a much less open structure and the EOC is expected to be dominated by the density of interfaces, i.e., by the concentration. Finally, we used the values of a and ξ to estimate the volumic fractions of polymer in the gels, using the simple model of a square network of cell parameter ξ made of polymer objects oriented along Z. We considered two kinds of polymer objects: (1) sheets of thickness a and (2) fibers of diameter a. The volumic fraction express $2a/\xi$ and $\pi a^2/4\xi^2$, respectively. The first model gives a good estimate of the real volumic fraction of polymer for all our samples. By contrast, the volumic fractions estimated from the second model are more than one order of magnitude smaller than the real values. Therefore, this simple calculation also supports the model of sheetlike polymer objects. In summary, we propose the schematic picture of Fig. 6 to describe the structure of nematic gels: the polymer forms sheets with a typical thickness a of a few tens of
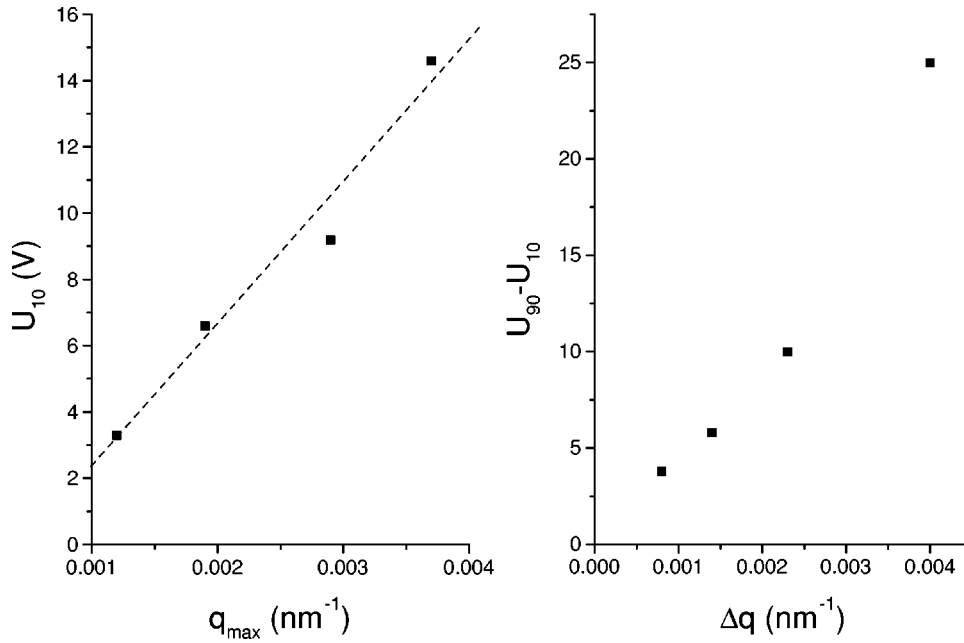
FIG. 14. Correlations between structure and electro-optical properties of the gels. U_{10} and U_{90} are defined in the text. (a) First threshold of the EOC as a function of position of scattering peak, the line is a guide for the eyes; (b) Difference between first and second thresholds of the EOC as a function of FWHM of the light scattering peak.

nm, probably swelled of LC, which entangle to form LC cavities with a correlation length ξ of a few μm. For high monomer concentrations and/or thick cells, both the polymer network and the nematic phase present an uniaxial symmetry with respect to the aligning direction. When the cell thickness is of the order of the correlation length, finite-size effects induce a preferential orientation of the polymer sheets perpendicular to the cell windows.

Finally, we discuss the relations between the structure and the electro-optical properties. The volumic fraction of anchored LC was shown to follow a voltage dependence similar to that followed by light transmission [13]. This is a direct evidence that the scattering contrast in nematic gels is between anchored and switched LC domains. It is also interesting to probe the relations between structure and EOC. Let us define U_{10} and U_{90} as the voltages corresponding to 10% and 90% loss of transmission, respectively, with respect to transmission in the *off* and *on* states. In Fig. 14(a), we reported the values of U_{10} as a function of $q_{0,max}$, the position of the scattering peak on the plateau, for gels prepared with monomer 4d. The data are well fitted by a linear dependence, which indicates that the electric field necessary to switch the LC is inversely proportional to ξ. This is temptating to compare this behavior to that of a pure nematic cell, where the electric field is inversely proportional to the thickness. This supports well the model of disconnected LC domains separated by polymer sheets, each domain playing the role of a small nematic cell. In Fig. 14(b), we study the correlations between U_{90}-U_{10} and the width of the scattering peak. The broader the width of the peak, the broader the range of voltage between the first and the last switched molecules. Note that no accurate quantitative analysis is allowed because of the possible contribution of multiple scattering to the peak

width. However, as already emphasized above, the broadening of the scattering peak also indicates an increase of polydispersity, and it is expected that switching spreads over a large range of voltages for polydisperse systems. This increase is particularly strong at high concentrations. For us, this is the signature of anchoring on polymer sheets that are perpendicular to the X direction. Since switching occurs in the plane XZ, the energy necessary for switching molecules anchored on polymer sheets parallel to the cell windows is much larger than that for polymer sheets perpendicular to the windows. Here again, these results support the pictures of Figs. 7, 8, and 11.

V. CONCLUSION

The structure of anisotropic nematic gels prepared in thin cells with uniform planar alignment was studied in optical microscopy, SANS, and light scattering from micrometer to nanometer scales. The results support the picture of thin sheets of polymer, which interconnect to form a network oriented along the alignment direction (Fig. 6). The structure is polydisperse, and the larger the monomer concentration, the larger the polydispersity. For small monomer concentrations and/or thin cells, finite-size effects lead to an orientation of the polymer sheets preferentially perpendicular to the cell windows (Fig. 11). The electro-optical properties of the gels are closely related to their structure.

[1] *Liquid Crystals in Complex Geometries*, edited by G.P. Crawford and S. Zumer (Taylor and Francis, London, 1996).

[2] For a review, see R.A.M. Hikmet, in *Liquid Crystals in Complex Geometries* (Ref. [1]), Chap. 3.

[3] J. Cognard, *Molecular Crystals and Liquid Crystals Supp. Series 1* (Gordon and Breach Science Publishers, New York, 1982).

[4] R.A.M. Hikmet and H.M.J. Boots, Phys. Rev. E **51**, 5824 (1995).

[5] R.A.M. Hikmet, J. Appl. Phys. **68**, 4410 (1990).

[6] R.A.M. Hikmet and R. Howard, Phys. Rev. E **48**, 2752 (1993).

[7] A. Riede, S. Grande, A. Hohmuth, and W. Weissflog, Liq. Cryst. **22**, 157 (1997).

[8] G.P. Crawford, A. Scharkowski, Y.K. Fung, J.W. Doane, and S. Zumer, Phys. Rev. E **52**, 1273 (1995); S. Zumer and G.P. Crawford, in *Liquid Crystals in Complex Geometries* (Ref. [1]), Chap. 4.

[9] D. Braun, G. Frick, M. Grell, M. Klimes, and J.H. Wendorff, Liq. Cryst. **11**, 929 (1992) (Ref. [16], Riede).

[10] A. Jàkli, D.R. Kim, L. Chien, and A. Saupe, J. Appl. Phys. **72**, 3161 (1992).

[11] A. Jàkli, L. Bata, K. Fodor-Csorba, L. Rosta, and L. Noirez, Liq. Cryst. **17**, 227 (1994); A. Jàkli, L. Rosta, and L. Noirez, *ibid.* **18**, 601 (1995).

[12] P. Gautier, Ph.D. thesis, Université Montpellier II, 1999.

[13] P. Gautier, M. Brunet, J. Grupp, J.L. Sauvajol, and E. Anglaret, Phys. Rev. E **62**, 7528 (2000).

[14] Y.K. Fung, D.K. Yang, L.C. Chien, S. Zumer, and J.W. Doane, Liq. Cryst. **19**, 797 (1995).

[15] I. Dierking, L.L. Kosbar, A. Afdali-Ardakani, A.C. Lowe, and G.A. Held, J. Appl. Phys. **81**, 3007 (1997); I. Dierking, L.L. Kosbar, A.C. Lowe, and G.A. Held, Liq. Cryst. **24**, 387 (1998).

[16] P. Gautier, M. Brunet, N. Basturk, and J. Grupp, Mol. Cryst. Liq. Cryst. **321**, 183 (1998).

[17] T. Zemb, in *Neutron, X-ray and Light Scattering*, edited by P. Lindner and T. Zemb (Elsevier Science Publishers, 1991), p. 177.

[18] L. Auvray and P. Auroy in *Neutron, X-ray and Light Scattering* (Ref. [17]), p. 199.